Report

Current Biology

Ecological diversification of a cyanobacterium through divergence of its novel chlorophyll *d*-based light-harvesting system

Highlights

- Functional divergence of the light-harvesting complex of *Acaryochloris marina*
- Three major photosynthetic spectral types identified by chlorophyll fluorescence
- Short- and long-wavelength types recently derived from an ancestral intermediate
- This resulted in specialization on different far-red wavelengths for photosynthesis

Authors

Nikea J. Ulrich, Gaozhong Shen, Donald A. Bryant, Scott R. Miller

Correspondence

scott.miller@umontana.edu

In brief

The evolution of novel traits has important consequences for biological diversification. Ulrich et al. show that the innovation of a new chlorophyll pigment by a cyanobacterium was followed by the functional divergence of its light-harvesting complex to specialize on different far-red wavelengths for photosynthesis.

Ulrich et al., 2024, Current Biology *34*, 1–8
July 8, 2024
https://doi.org/10.1016/j.cub.2024.05.022

CellPress

Current Biology

CellPress

Report

Ecological diversification of a cyanobacterium through divergence of its novel chlorophyll *d*-based light-harvesting system

Nikea J. Ulrich,[1] Gaozhong Shen,[2] Donald A. Bryant,[2] and Scott R. Miller[1,3,*]
[1]Division of Biological Sciences, University of Montana, 32 Campus Drive, Missoula, MT 59812, USA
[2]Department of Biochemistry and Molecular Biology, Pennsylvania State University, 406 Althouse Lab, University Park, PA 16802, USA
[3]Lead contact
*Correspondence: scott.miller@umontana.edu
https://doi.org/10.1016/j.cub.2024.05.022

SUMMARY

The evolution of novel traits can have important consequences for biological diversification. Novelties such as new structures are associated with changes in both genotype and phenotype that often lead to changes in ecological function.[1,2] New ecological opportunities provided by a novel trait can trigger subsequent trait modification or niche partitioning[3]; however, the underlying mechanisms of novel trait diversification are still poorly understood. Here, we report that the innovation of a new chlorophyll (Chl) pigment, Chl *d*, by the cyanobacterium *Acaryochloris marina* was followed by the functional divergence of its light-harvesting complex. We identified three major photosynthetic spectral types based on Chl fluorescence properties for a collection of *A. marina* laboratory strains for which genome sequence data are available,[4,5] with shorter- and longer-wavelength types more recently derived from an ancestral intermediate phenotype. Members of the different spectral types exhibited extensive variation in the Chl-binding proteins as well as the Chl energy levels of their photosynthetic complexes. This spectral-type divergence is associated with differences in the wavelength dependence of both growth rate and photosynthetic oxygen evolution. We conclude that the divergence of the light-harvesting apparatus has consequently impacted *A. marina* ecological diversification through specialization on different far-red photons for photosynthesis.

RESULTS AND DISCUSSION

Divergence of *A. marina* photosynthetic spectral types from an intermediate ancestor

Novel traits are engines of biological diversification. The evolution of a novel trait can enable an organism to access unoccupied niches where there are new resources to exploit,[6–8] which can trigger an adaptive radiation through subsequent trait modification.[3,9] During the process of novel trait diversification, populations might begin to partition the new niche space to avoid intraspecific competition.[10] This partitioning may be temporal,[11,12] spatial,[13] or with respect to resource utilization.[10] The latter involves character displacement, i.e., an evolutionary change in a trait that enables specialization on a specific resource.[14] However, despite the importance of novel traits, with few exceptions (e.g., Erwin[15] and Mallarino et al.[16]) we rarely know their underlying mechanisms of diversification.

One of the most consequential innovations in the history of life was the invention of chlorophyll (Chl) *a*-based photosynthesis by cyanobacteria, which sparked the oxygenation of Earth. Since the origin of Chl *a* and its subsequent acquisition by diverse eukaryotes via endosymbiosis, different organisms have extended the reach of the photosynthetic apparatus through the diversification of light-harvesting complexes (LHCs) that harvest wavelengths of light that are inaccessible to Chl *a*. While photosynthetic reaction center structure, composition, and function have been highly conserved during billions of years of Chl *a*-based oxygenic photosynthesis,[17] spectrally distinct LHCs have independently evolved in diverse photosynthetic lineages over the same period of time. These independently derived LHCs include the phycobilisomes (PBSs) of most cyanobacteria and red algae,[18,19] the prochlorophyte Chl *a*/*b*-binding proteins (Pcb),[20] the LHC proteins of green algae and plants,[21,22] and the fucoxanthin Chl *a*/*c*-binding proteins of stramenopiles and haptophytes.[23,24] LHCs are often tuned to specialize on the prevailing light available in the environment[25] (e.g., the diversity of PBS pigments in marine *Synechococcus* at varying depths). Many plants and cyanobacteria also contain small proportions of long-wavelength (LW)-absorbing Chl *a* molecules (red Chls) associated with photosystem I (PSI) to extend their light-harvesting capacity in shaded environments.[26,27] However, due to the ancient origins of Chl *a*-based photosynthetic systems, it is difficult to reconstruct the evolutionary history of Chl *a*-based LHC diversification.

By contrast, the comparatively recent origin of Chl *d* tens of millions of years ago in the cyanobacterium *Acaryochloris marina*[28–30] offers the rare opportunity to investigate the process of LHC diversification following the innovation of a novel Chl pigment. Chl *d* differs from Chl *a* by the replacement of a vinyl group with a formyl group at the C-3 position of the chlorin

Please cite this article in press as: Ulrich et al., Ecological diversification of a cyanobacterium through divergence of its novel chlorophyll *d*-based light-harvesting system, Current Biology (2024), https://doi.org/10.1016/j.cub.2024.05.022

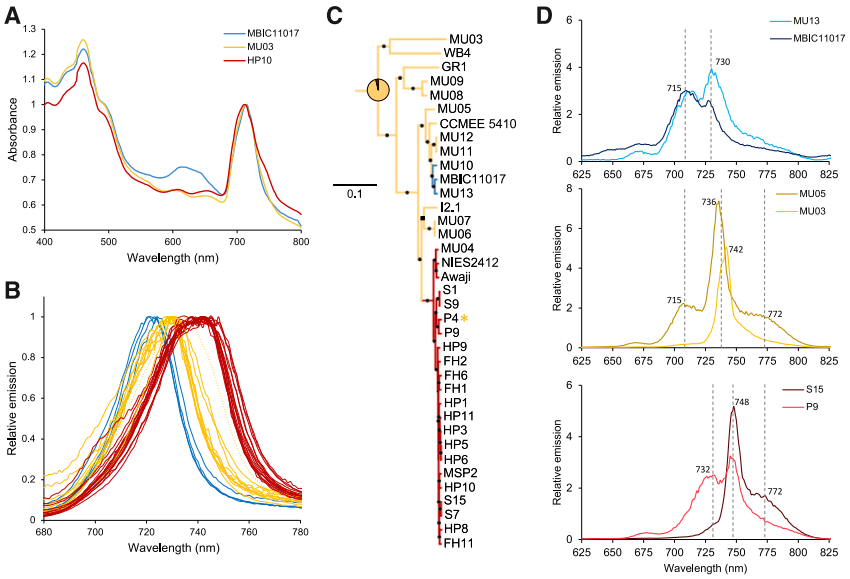

Figure 1. Divergence of *A. marina* photosynthetic spectral types

Data are color coded by spectral type in all panels.

(A) *In vivo* absorption spectra of representative strains MBIC11017, MU03, and HP10 normalized by the Chl *d* peak (713 nm).

(B) RT fluorescence emission spectra of *A. marina* strains grown in white light. P4 emission spectrum indicated by dotted yellow line.

(C) Maximum likelihood phylogeny of *A. marina* strains adapted from Miller et al.,[4] which was outgroup rooted with *A. thomasi* RCC1774. Branch lengths are in units of the expected number of amino acid substitutions per site. Bootstrap support was >98% for nodes indicated by black squares and 100% for nodes indicated by black circles. The asterisk by P4 indicates an intermediate phenotype between LW and IW. Ancestral state reconstruction by the marginal posterior probabilities approximation (MPPA) maximum likelihood model and F81 model for character evolution indicates 99.4% marginal posterior probability of IW as the ancestral state, indicated by the pie chart.

(D) 77 K fluorescence emission spectra of whole cells from select strains of each spectral type. Dotted lines indicate peaks.

See also Figures S1, S2, and S4.

ring, which shifts pigment absorption into the far-red (FR) spectral region (700–750 nm[28]). In *A. marina*, Chl *d* constitutes >90% of Chl content, including the reaction center Chls where photochemistry occurs.[31] This enables *A. marina* to thrive in low-light, low-energy habitats, and it is widely distributed in shallow temperate and tropical saline environments where visible light is filtered, often attached to red algae or animals.[4] Like prochlorophyte cyanobacteria, *A. marina* and its close relative *A. thomasi*, which does not produce Chl *d*,[32] use membrane-bound Pcb proteins for light harvesting.[33,34] Yet it remains unknown whether the innovation of Chl *d* has been followed by the diversification of the *A. marina* LHC to specialize on different FR wavelengths, as predicted by niche-partitioning theory. Resolving this question has implications for our understanding of the process of biological diversification after the origin of a novel trait.

To investigate LHC functional diversity, we first obtained room temperature (RT) absorption and fluorescence emission spectra for a sample of 30 *A. marina* laboratory strains isolated from diverse geographic locations and grown in a white light environment.[4,5] The absorption spectra of strains were very similar (Figure S1), including the characteristic Q_y peak of Chl *d* at 710–715 nm, and pigment composition is qualitatively identical among strains with respect to the kinds of Chl and carotenoid pigments produced (Chl *d* with small amounts of Chl *a* and pheophytin *a*, α-carotene, and zeaxanthin; Figure S1). However, Figure 1A highlights key differences observed for representative strains. Strain HP10 exhibited an additional shoulder of LW absorbance at ~740–750 nm, compared with strains MBIC11017 and MU03 (Figure 1A), which was also recently observed for the *A. marina* strain Moss Beach.[35] This variation in Chl *d* absorption suggests functional differences in light use across *A. marina* strains. Meanwhile, the type-strain MBIC11017, which is the only *A. marina* strain known to produce the light-harvesting pigment phycocyanin,[5] additionally produced an absorption peak for this phycobiliprotein at ~620 nm (Figure 1A[36]), obscuring the Q_x bands of Chl at 605 and 650 nm (Figure 1A).

We next characterized RT fluorescence emission spectra, which detect photons radiated by excited electrons of light-harvesting antenna Chl molecules as they return to ground state (particularly the photosystem II [PSII] antenna when performed at RT[37]). Differences among strains were more apparent for RT fluorescence emission compared with absorption (Figure 1B). We identified three major *A. marina* spectral types: a previously unidentified intermediate wavelength (IW) type with an emission maximum at 727–731 nm; a short-wavelength (SW) spectral type with an emission maximum at 721–724 nm, as reported for *A. marina* strain MBIC11017[36]; and a LW spectral type with a broader emission peak and maximum at 738–748 nm, first observed for *A. marina* strain Awaji.[38]

Many photosynthetic organisms have the capacity to adjust the composition of their light-harvesting systems to better match the quality of light in the environment by a process called complementary chromatic acclimation (CCA[39]). Several CCA mechanisms have been characterized in cyanobacteria.[40,41] To address whether differences in CCA could explain the different *A. marina* spectral types, we grew strains at different light intensities in both white and FR light. Although strains did exhibit minor shifts in fluorescence emission maximum in response to changes in light quantity and quality, strains consistently remained in the same spectral-type grouping irrespective of light environment (Figure S2). We conclude that the *A. marina* spectral types are due to fixed, evolved differences among strains rather than the product of differences in acclimation response.

To understand the evolutionary origins of the divergent spectral types, we mapped the RT fluorescence emission

Please cite this article in press as: Ulrich et al., Ecological diversification of a cyanobacterium through divergence of its novel chlorophyll *d*-based light-harvesting system, Current Biology (2024), https://doi.org/10.1016/j.cub.2024.05.022

phenotype onto a genome-wide *A. marina* phylogeny (Figure 1C[4]). Members of the earliest branching lineages exhibited the IW spectral type, indicating that this was most likely the ancestral phenotype. Ancestral state reconstruction (ASR) by the marginal posterior probabilities approximation (MPPA) maximum likelihood model and F81 model for character evolution strongly supports this hypothesis (99.4% marginal posterior probability). Strikingly, the derivations of both SW and LW spectral types through hypsochromic and bathochromic shifts in fluorescence wavelengths, respectively, appear to be comparatively recent (Figure 1C). The SW spectral type (observed in strains MU13, MBIC11017, and MU10) originated within a clade of primarily tunicate-associated *A. marina* (Figure 1C[4]), whereas the LW spectral type was innovated by the ancestor of a clade of strains isolated from diverse locations, including western North America, Portugal, Italy, and Japan. One strain (P4) exhibits an intermediate phenotype between LW and IW spectral types, suggesting a partial reversion to the ancestral phenotype (Figures 1B, 1C, and S4).

Possible sources of functional variation among *A. marina* spectral types

The observed differences in RT fluorescence emission maxima among spectral types suggest the presence of different energy forms of Chl in the light-harvesting apparatus,[37] which impacts the wavelengths of photons that are harvested as well as the flow of excitation energy to the reaction centers.[42,43] To investigate this in more detail, we obtained 77 K fluorescence emission spectra, which better resolve functional differences among photosynthetic systems by eliminating biochemical and physiological processes, slowing down energy transfer and sharpening peaks through the loss of intramolecular vibrations.[37] 77 K spectra corroborated RT observations of differences among spectral types in Chl energy levels but also revealed variation within each spectral type that was not apparent for PSII-dominated RT fluorescence (Figure 1D). Both SW and IW spectral types contained a 715-nm and a prominent ~730-nm emission peak; however, the latter peak was shifted to longer wavelengths in IW strains (ranging from 736 to 742 nm) (Figure 1D). MU05 had an additional emission shoulder at 772 nm as well as the 715-nm peak, both of which MU03 (earliest branching *A. marina* strain) lacked (Figure 1D). This was also the case for LW strains, yet both S15 and P4 contained a longer-wavelength shift of the prominent peak to 748 nm (Figure 1D).

Although a detailed characterization of the mechanisms that give rise to this rich functional variation within and between *A. marina* spectral types is the subject of future work, we identified possible contributors to these patterns, which are not mutually exclusive. Because the different spectral types use the same kinds of Chls and carotenoids (Figure S1), differences among spectral types are likely due to (1) changes in protein environment (e.g., hydrophobicity) in the vicinity of Chl molecules that are caused by variability in Pcb sequence and/or composition within LHCs and/or (2) differences in the amounts of Chl *d* versus Chl *a* molecules in the light-harvesting antenna proteins themselves.

A. marina pcb genes are members of a large gene family that includes prochlorophyte *pcb*, the iron-stress gene *isiA* and the *psbC* and *psbB* genes of PSII (Figure S3[44,45]) Whereas *A. marina pcbA* genes are more closely related to *isiA*, *pcbC* paralogs form a separate clade; all are derived from three ancestral copies with orthologs in *A. thomasi* RCC1774 (Figures 2 and S3), most likely obtained by ancient horizontal transfer from prochlorophyte(s). *A. marina* strains exhibit extensive variation in *pcb* copy number (ranging from 6 to 10 copies; Figure 2A) due to a dynamic history of gene duplication, differential retention of paralogs, and horizontal acquisition of genes from other *A. marina* strains (Figure 2). Basal *A. marina* lineages diverged prior to several *pcb* duplication events and consequently harbor fewer gene copies (Figures 2A and 2B), which is associated with fewer fluorescence emission peaks (Figure 1D).

Although the same *pcb* repertoire is generally shared within each spectral type (Figure 2A), recombination of *pcb* alleles during *A. marina* diversification may contribute to spectral differences between closely related strains. For example, strains P4 and P9 possess the same number and kinds of Pcbs (Figure 2A), but P4 alleles for two *pcbA* loci are more closely related to those of basal strains than LW strains (Figure S4). This may contribute to the unique RT fluorescence emission spectrum of strain P4, which is intermediate between ancestral and LW spectral types (Figures 1B and S4).

Differences in Pcb stoichiometry may also contribute to functional differences of *A. marina* LHC. We purified Chl-protein complexes of selected strains by sucrose density gradient centrifugation (Figure 3A) and characterized fluorescence properties of specific fractions. Fraction F3 primarily contained PSI complexes based on position in the density gradient and similarity of pigment absorption and emission compared with published results for iron-replete MBIC11017.[34,46,47] Notably, the F3 absorption spectrum for SW strain MBIC11017 is missing a prominent longer-wavelength shoulder that is observed in MU05 and P4 (Figure 3B); this FR shoulder was further resolved at 77 K as a broad band of intense fluorescence emission at wavelengths greater than 750 nm, which was absent in MBIC11017 (Figure 3C). This broad bandwidth suggests the presence of multiple Chl molecules with lower energy than the PSI reaction center[48] (peak wavelength of 740 nm = 1.68 eV), which would necessitate thermally activated uphill energy transfer from the antenna to the PSI special pair. Low-energy Chl *a* molecules (red Chls) within other cyanobacterial PSI antenna have been shown to be involved in light harvesting (reviewed in Karapetyan et al.[49]). Liquid chromatography-mass spectrometry (LC-MS) analysis of F3 for MBIC11017 and MU05 showed enrichment of PSI proteins together with multiple Pcb proteins. The Pcbs of MBIC11017 (SW) were dominated by PcbA1 paralogs 1369 and 3654 (MBIC11017 numbering; Table S1; Figure 2C). PcbA1 3654 expressed in Chl *a*-producing *Synechocystis* sp. PCC 6803 exhibits a 723-nm emission peak at 77 K[50]; we therefore assigned the MBIC11017 emission band at 729 nm (red-shifted due to the presence of Chl *d*) to these PcbA1 copies. By contrast, F3 of MU05 contained similar amounts of PcbC copies 1368/3655 (these paralogs have identical sequences) compared with 1369 and 3654 (Table S2). These Pcbs may therefore be responsible for the LW fluorescence that is absent in MBIC11017, and the transition from IW to SW spectral types most likely involved evolved differences in Pcb stoichiometry of the PSI LHC.

Please cite this article in press as: Ulrich et al., Ecological diversification of a cyanobacterium through divergence of its novel chlorophyll *d*-based light-harvesting system, Current Biology (2024), https://doi.org/10.1016/j.cub.2024.05.022

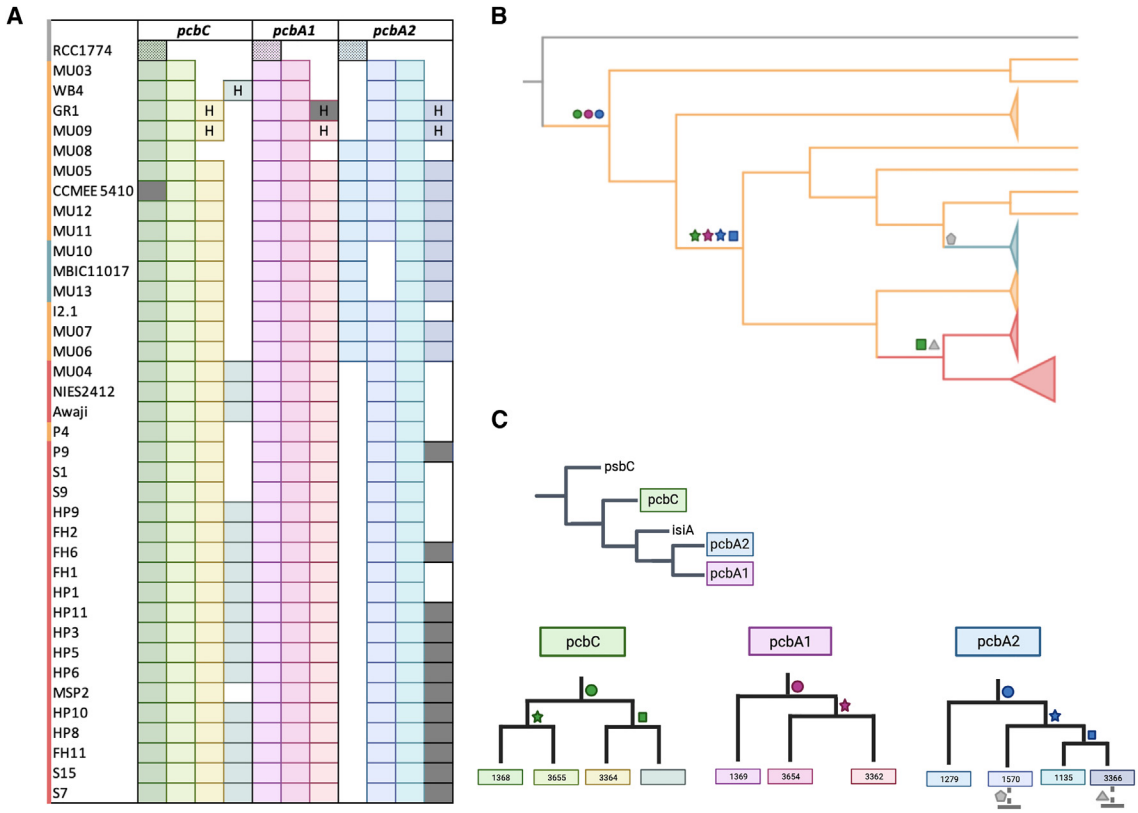

Figure 2. Pcb copy-number variation and complex evolution in *Acaryochloris*

(A) Presence/absence table of *pcb* gene copies in *Acaryochloris* strains. Strains are color coded by spectral type and are ordered as in Figure 1C. Gray boxes indicate pseudogenes and white boxes indicate the absence of a gene copy. Horizontally acquired genes, identified by phylogenetic analysis, are indicated by "H."

(B) Partially collapsed *Acaryochloris* phylogeny outgroup rooted with *A. thomasi* RCC1774 (gray). *A. marina* branches are colored by identified spectral type. Green (*pcbC*), pink (*pcbA1*), and blue (*pcbA2*) symbols indicate an inferred duplication, gray symbols indicate an inferred loss, as in (C).

(C) Collapsed gene tree of all *pcb* copies and inferred gene trees of *pcbC*, *pcbA1*, and *pcbA2* copies. Genes are labeled using MBIC11017 numbering, except for pcbA2 copy 1570 (which MBIC11017 lacks). Green, pink, and blue symbols indicate an inferred duplication; gray symbols indicate an inferred loss, as in (B). See also Figure S3.

Finally, evolved differences in the amounts of Chl *d* versus Chl *a* in light-harvesting antenna proteins may have contributed to the transition from IW to SW spectral types (Figure 1C). SW strains MBIC11017 and MU13 exhibit a lower pheophytin *a*-normalized Chl *d*: Chl *a* (mean ± SE; 7.61 ± 1.23) than IW and LW strains (13.7 ± 0.14; Figure 3D). This increase in antenna Chl *a* molecules in SW strains is evident as enhanced Chl fluorescence emission at wavelengths below 700 nm (Figure 1D).

Physiological and fitness consequences of spectral-type divergence

Do these differences in spectral type have phenotypic consequences, such as specialization on different FR wavelengths? We predicted that a basal *A. marina* strain with ancestral spectral type would be an FR generalist. By contrast, during the process of diversification, cells might subsequently have partitioned ecological niche space through spectral-type divergence and specialization on specific FR wavelengths as a response to new ecological opportunities or competition avoidance with other *A. marina*.[51,52] To investigate this, we compared growth rates and photosynthetic oxygen production of representative strains from each spectral type in different FR environments provided by LED sources with peak emission at 706 nm (approximately the Chl *d in vivo* absorption maximum) and 731 nm, respectively.

Strains responded to the light environments differently (Figure 4A), as indicated by a highly significant strain x light interaction term in a linear model ($F_{2,15} = 12.43$; $p = 0.001$). Specifically, basal IW strain MU03 exhibited no difference in growth rate between light environments ($F_{1,4} = 0.30$; $p = 0.62$; Figure 4A), as expected for an intermediate generalist phenotype. By contrast, derived spectral types exhibited growth patterns consistent with predictions based on evolved shifts in Chl fluorescence (Figure 4A): HP10 (LW) grew significantly slower in 706 nm compared with 731 nm ($F_{1,4} = 17.2$; $p = 0.01$), whereas the growth rate for MU13 (SW) was faster in 706 nm ($F_{1,4} = 6.02$; $p = 0.07$). Observed differences in absolute performance among strains may reflect phenotypic differences with respect to their responses to other environmental parameters in the growth assay (e.g., temperature and light intensity). With respect to photosynthetic oxygen evolution, LW strain HP10 exhibited a much lower rate at 706 nm (Figure 4B; $F_{2,27} = 4.91$, $p = 0.016$

Please cite this article in press as: Ulrich et al., Ecological diversification of a cyanobacterium through divergence of its novel chlorophyll *d*-based light-harvesting system, Current Biology (2024), https://doi.org/10.1016/j.cub.2024.05.022

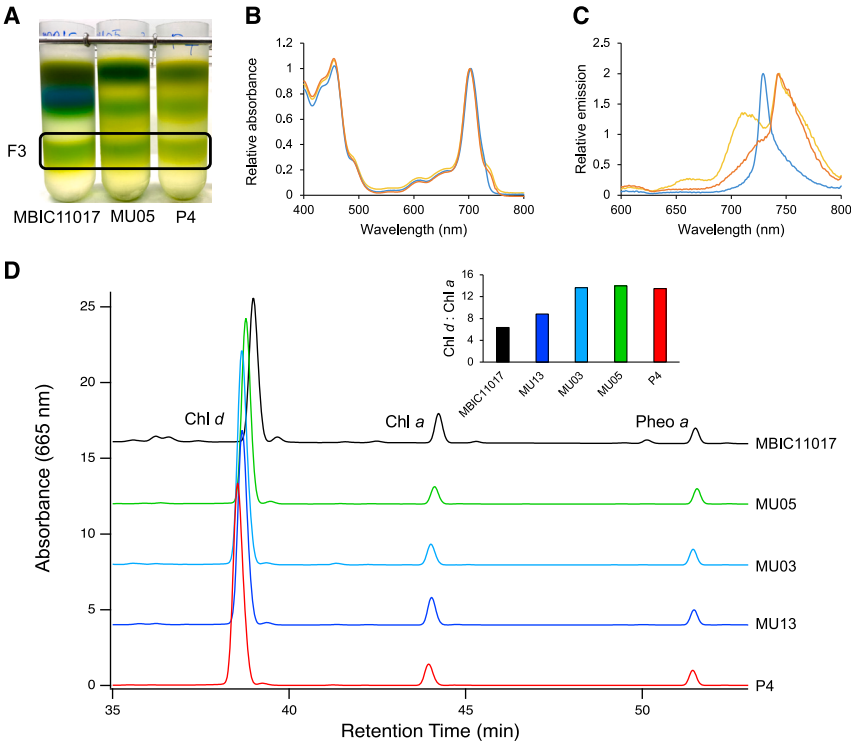

Figure 3. Possible contributors to derived shifts in *A. marina* spectral types

(A–C) (A) Fractions of Chl-protein complexes from MBIC11017, MU05, and P4 after sucrose density gradient centrifugation. Fraction 3 (F3) was further purified, and absorption (B) and 77 K fluorescence emission (C) spectra were performed for F3 fractions of MU05 (yellow), MBIC11017 (blue), and P4 (orange).

(D) High-performance liquid chromatography chromatogram of *A. marina* strains MBIC11017, MU05, MU03, MU13, and P4 normalized to pheophytin *a*. Minor differences in retention times are not due to chemical difference: spectra of eluted pigments were compared with standards authenticated by LC-MS to verify identities. Inset: estimated ratios of Chl *d*:Chl *a*, when normalized to pheophytin *a*.

See also Tables S1 and S2.

for the strain × light interaction term) than either MU03 (IW) or MU13 (SW). The low net rates of oxygen evolution for HP10 in 706 nm light might explain, in part, the reduced growth rate we observed at shorter wavelengths.

Taken together, *A. marina* spectral types exhibit physiological differences when grown in different FR light environments, suggesting that derived spectral types have specialized to use distinct FR wavelength environments. Divergence of *A. marina* spectral types therefore resembles the diversification of beak size and shape in Darwin's finches that is associated with specialization on different diets.[53] Although we cannot infer the environment in which these spectral types were derived, *A. marina* strains of different spectral types are known to co-occur in nature (e.g., P4/P9 and MU03/MU04[4]). Consequently, we speculate that resource partitioning of available light wavelengths was favored by *A. marina* strains for competition avoidance. Future investigations could try to resolve the variation in light environments between *A. marina* spectral types in nature. We conclude that, following the innovation of a Chl *d*-based light-harvesting system in *A. marina*, ecological divergence has enabled strains to preferentially use different FR wavelengths for photosynthesis.

STAR★METHODS

Detailed methods are provided in the online version of this paper and include the following:

- KEY RESOURCES TABLE
- RESOURCE AVAILABILITY
  - Lead contact

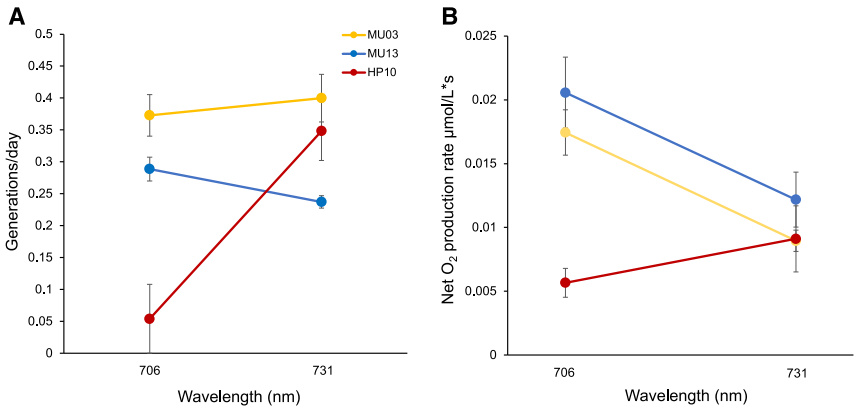

Figure 4. Physiological and fitness consequences of spectral-type divergence

Error bars are standard errors.

(A) Population growth rates in 706 and 731 nm FR light environments for MU03 (IW, yellow), MU13 (SW, blue), and HP10 (LW, red).

(B) Net rates of oxygen production for MU03, MU13, and HP10 when grown and assayed in 706 and 731 nm, respectively.

SUPPLEMENTAL INFORMATION

Supplemental information can be found online at https://doi.org/10.1016/j.cub.2024.05.022.

ACKNOWLEDGMENTS

We thank Heidi Abresch and Nathan Miller for their help maintaining *Acaryochloris* cultures at the University of Montana and Dr. Tatiana N. Laremore at The Pennsylvania State University for assistance with peptide fingerprint analyses by mass spectroscopy. This work was supported by award NNA15BB04A from the National Aeronautics and Space Administration to S.R.M. N.J.U. was supported by the P.E.O. Scholar Award, Montana Space Grant Fellowship, and University of Montana's Dissertation Completion Fellowship. Research in the laboratory of D.A.B. was supported by the National Science Foundation grant MCB-1613022.

AUTHOR CONTRIBUTIONS

Conceptualization, N.J.U. and S.R.M.; methodology, N.J.U., G.S., D.A.B., and S.R.M.; investigation, N.J.U., G.S., and S.R.M.; writing – original draft, N.J.U.; writing – review & editing, S.R.M., N.J.U., G.S., and D.A.B.; funding acquisition, S.R.M., D.A.B., and N.J.U.; resources, S.R.M. and D.A.B.; supervision, S.R.M.

DECLARATION OF INTERESTS

The authors declare no competing interests.

Received: March 27, 2024
Revised: May 7, 2024
Accepted: May 13, 2024
Published: June 7, 2024

REFERENCES

1. Galis, F., and Metz, J.A.J. (2007). Evolutionary novelties: the making and breaking of pleiotropic constraints. Integr. Comp. Biol. *47*, 409–419. https://doi.org/10.1093/icb/icm081.
2. Wagner, G.P., and Lynch, V.J. (2010). Evolutionary novelties. Curr. Biol. *20*, R48–R52. https://doi.org/10.1016/j.cub.2009.11.010.
3. Schluter, D. (2000). Ecological character displacement in adaptive radiation. Am. Nat. *156*, S4–S16. https://doi.org/10.1086/303412.
4. Miller, S.R., Abresch, H.E., Baroch, J.J., Fishman Miller, C.K.F., Garber, A.I., Oman, A.R., and Ulrich, N.J. (2022). Genomic and functional variation of the chlorophyll d-producing cyanobacterium *Acaryochloris marina*. Microorganisms *10*, 569. https://doi.org/10.3390/microorganisms10030569.
5. Ulrich, N.J., Uchida, H., Kanesaki, Y., Hirose, E., Murakami, A., and Miller, S.R. (2021). Reacquisition of light-harvesting genes in a marine cyanobacterium confers a broader solar niche. Curr. Biol. *31*, 1539–1546.e4. https://doi.org/10.1016/j.cub.2021.01.047.
6. Rabosky, D.L. (2017). Phylogenetic tests for evolutionary innovation: the problematic link between key innovations and exceptional diversification. Philos. Trans. R. Soc. Lond. B Biol. Sci. *372*, 20160417. https://doi.org/10.1098/rstb.2016.0417.
7. Garcia-Porta, J., and Ord, T.J. (2013). Key innovations and island colonization as engines of evolutionary diversification: a comparative test with the Australasian diplodactyloid geckos. J. Evol. Biol. *26*, 2662–2680. https://doi.org/10.1111/jeb.12261.
8. Miller, A.H., Stroud, J.T., and Losos, J.B. (2023). The ecology and evolution of key innovations. Trends Ecol. Evol. *38*, 122–131. https://doi.org/10.1016/j.tree.2022.09.005.
9. Emlen, D.J., Corley Lavine, L., and Ewen-Campen, B. (2007). On the origin and evolutionary diversification of beetle horns. Proc. Natl. Acad. Sci. USA *104*, 8661–8668. https://doi.org/10.1073/pnas.0701209104.
10. Schoener, T.W. (1974). Resource partitioning in ecological communities: research on how similar species divide resources helps reveal the natural regulation of species diversity. Science *185*, 27–39. https://doi.org/10.1126/science.185.4145.27.
11. Kronfeld-Schor, N., and Dayan, T. (2003). Partitioning of time as an ecological resource. Annu. Rev. Ecol. Evol. Syst. *34*, 153–181. https://doi.org/10.1146/annurev.ecolsys.34.011802.132435.
12. Monterroso, P., Alves, P.C., and Ferreras, P. (2014). Plasticity in circadian activity patterns of mesocarnivores in Southwestern Europe: implications for species coexistence. Behav. Ecol. Sociobiol. *68*, 1403–1417. https://doi.org/10.1007/s00265-014-1748-1.
13. Jablonski, P.G., Borowiec, M., Nowakowski, J.J., and Stawarczyk, T. (2020). Ecological niche partitioning in a fragmented landscape between two highly specialized avian flush-pursuit foragers in the Andean zone of sympatry. Sci. Rep. *10*, 22024. https://doi.org/10.1038/s41598-020-78804-2.
14. Pfennig, K.S., and Pfennig, D.W. (2009). Character displacement: ecological and reproductive responses to a common evolutionary problem. Q. Rev. Biol. *84*, 253–276. https://doi.org/10.1086/605079.
15. Erwin, D.H. (2015). Novelty and innovation in the history of life. Curr. Biol. *25*, R930–R940. https://doi.org/10.1016/j.cub.2015.08.019.
16. Mallarino, R., Grant, P.R., Grant, B.R., Herrel, A., Kuo, W.P., and Abzhanov, A. (2011). Two developmental modules establish 3D beak-shape variation in Darwin's finches. Proc. Natl. Acad. Sci. USA *108*, 4057–4062. https://doi.org/10.1073/pnas.1011480108.
17. Nelson, N., and Junge, W. (2015). Structure and energy transfer in photosystems of oxygenic photosynthesis. Annu. Rev. Biochem. *84*, 659–683. https://doi.org/10.1146/annurev-biochem-092914-041942.
18. MacColl, R. (1998). Cyanobacterial phycobilisomes. J. Struct. Biol. *124*, 311–334. https://doi.org/10.1006/jsbi.1998.4062.
19. Chang, L., Liu, X., Li, Y., Liu, C.C., Yang, F., Zhao, J., and Sui, S.F. (2015). Structural organization of an intact phycobilisome and its association with photosystem II. Cell Res. *25*, 726–737. https://doi.org/10.1038/cr.2015.59.
20. La Roche, J., Van Der Staay, G.W.M., Partensky, F., Ducret, A., Aebersold, R., Li, R., Golden, S.S., Hiller, R.G., Wrench, P.M., Larkum, A.W.D., et al. (1996). Independent evolution of the prochlorophyte and green plant chlorophyll *a*/*b* light-harvesting proteins. Proc. Natl. Acad. Sci. USA *93*, 15244–15248. https://doi.org/10.1073/pnas.93.26.15244.
21. Green, B.R., and Durnford, D.G. (1996). The chlorophyll-carotenoid proteins of oxygenic photosynthesis. Annu. Rev. Plant Physiol. Plant Mol. Biol. *47*, 685–714. https://doi.org/10.1146/annurev.arplant.47.1.685.
22. Neilson, J.A.D., and Durnford, D.G. (2010). Structural and functional diversification of the light-harvesting complexes in photosynthetic eukaryotes. Photosynth. Res. *106*, 57–71. https://doi.org/10.1007/s11120-010-9576-2.
23. Bhaya, D., and Grossman, A.R. (1993). Characterization of gene clusters encoding the fucoxanthin chlorophyll proteins of the diatom *Phaeodactylum tricornutum*. Nucl. Acids Res. *21*, 4458–4466. https://doi.org/10.1093/nar/21.19.4458.
24. Wang, W., Yu, L.-J., Xu, C., Tomizaki, T., Zhao, S., Umena, Y., Chen, X., Qin, X., Xin, Y., Suga, M., et al. (2019). Structural basis for blue-green light

harvesting and energy dissipation in diatoms. Science *363*, eaav0365. https://doi.org/10.1126/science.aav0365.

25. Grébert, T., Garczarek, L., Daubin, V., Humily, F., Marie, D., Ratin, M., Devailly, A., Farrant, G.K., Mary, I., Mella-Flores, D., et al. (2022). Diversity and evolution of pigment types in marine *Synechococcus* cyanobacteria. Genome Biol. Evol. *14*, evac035. https://doi.org/10.1093/gbe/evac035.
26. Bína, D., Durchan, M., Kuznetsova, V., Vácha, F., Litvín, R., and Polívka, T. (2019). Energy transfer dynamics in a red-shifted violaxanthin-chlorophyll a light-harvesting complex. Biochim. Biophys. Acta Bioenerg. *1860*, 111–120. https://doi.org/10.1016/j.bbabio.2018.11.006.
27. Herbstová, M., Bína, D., Kaňa, R., Vácha, F., and Litvín, R. (2017). Red-light phenotype in a marine diatom involves a specialized oligomeric red-shifted antenna and altered cell morphology. Sci. Rep. *7*, 11976. https://doi.org/10.1038/s41598-017-12247-0.
28. Miyashita, H., Ikemoto, H., Kurano, N., Adachi, K., Chihara, M., and Miyachi, S. (1996). Chlorophyll d as a major pigment. Nature *383*, 402. https://doi.org/10.1038/383402a0.
29. Swingley, W.D., Chen, M., Cheung, P.C., Conrad, A.L., Dejesa, L.C., Hao, J., Honchak, B.M., Karbach, L.E., Kurdoglu, A., Lahiri, S., et al. (2008). Niche adaptation and genome expansion in the chlorophyll d-producing cyanobacterium *Acaryochloris marina*. Proc. Natl. Acad. Sci. USA *105*, 2005–2010. https://doi.org/10.1073/pnas.0709772105.
30. Miller, S.R., Augustine, S., Olson, T.L., Blankenship, R.E., Selker, J., and Wood, A.M. (2005). Discovery of a free-living chlorophyll d-producing cyanobacterium with a hybrid proteobacterial/cyanobacterial small-subunit rRNA gene. Proc. Natl. Acad. Sci. USA *102*, 850–855. https://doi.org/10.1073/pnas.0405667102.
31. Larkum, A.W.D., and Kühl, M. (2005). Chlorophyll d: the puzzle resolved. Trends Plant Sci. *10*, 355–357. https://doi.org/10.1016/j.tplants.2005.06.005.
32. Partensky, F., Six, C., Ratin, M., Garczarek, L., Vaulot, D., Probert, I., Calteau, A., Gourvil, P., Marie, D., Grébert, T., et al. (2018). A novel species of the marine cyanobacterium *Acaryochloris* with a unique pigment content and lifestyle. Sci. Rep. *8*, 9142. https://doi.org/10.1038/s41598-018-27542-7.
33. Li, Z.K., Yin, Y.C., Zhang, L.D., Zhang, Z.C., Dai, G.Z., Chen, M., and Qiu, B.S. (2018). The identification of IsiA proteins binding chlorophyll d in the cyanobacterium *Acaryochloris marina*. Photosynth. Res. *135*, 165–175. https://doi.org/10.1007/s11120-017-0379-6.
34. Chen, M., Hiller, R.G., Howe, C.J., and Larkum, A.W.D. (2005). Unique origin and lateral transfer of prokaryotic chlorophyll-*b* and chlorophyll-*d* light-harvesting systems. Mol. Biol. Evol. *22*, 21–28. https://doi.org/10.1093/molbev/msh250.
35. Kiang, N.Y., Swingley, W.D., Gautam, D., Broddrick, J.T., Repeta, D.J., Stolz, J.F., Blankenship, R.E., Wolf, B.M., Detweiler, A.M., Miller, K.A., et al. (2022). Discovery of chlorophyll d: isolation and characterization of a far-red cyanobacterium from the original site of Manning and Strain (1943) at Moss Beach, California. Microorganisms *10*, 819. https://doi.org/10.3390/microorganisms10040819.
36. Murakami, A., Miyashita, H., Iseki, M., Adachi, K., and Mimuro, M. (2004). Chlorophyll d in an epiphytic cyanobacterium of red algae. Science *303*, 1633. https://doi.org/10.1126/science.1095459.
37. Lamb, J.J., Røkke, G., and Hohmann-Marriott, M.F. (2018). Chlorophyll fluorescence emission spectroscopy of oxygenic organisms at 77 K. Photosynthetica *56*, 105–124. https://doi.org/10.1007/s11099-018-0791-y.
38. Akimoto, S., Murakami, A., Yokono, M., Koyama, K., Tsuchiya, T., Miyashita, H., Yamazaki, I., and Mimuro, M. (2006). Fluorescence properties of the chlorophyll d-dominated cyanobacterium *Acaryochloris* sp. strain Awaji. J. Photochem. Photobiol. A *178*, 122–129. https://doi.org/10.1016/j.jphotochem.2005.09.031.
39. Anderson, J.M., Chow, W.S., and Park, Y.I. (1995). The grand design of photosynthesis: acclimation of the photosynthetic apparatus to environmental cues. Photosynth. Res. *46*, 129–139. https://doi.org/10.1007/BF00020423.
40. Gutu, A., and Kehoe, D.M. (2012). Emerging perspectives on the mechanisms, regulation, and distribution of light color acclimation in cyanobacteria. Mol. Plant *5*, 1–13. https://doi.org/10.1093/mp/ssr054.
41. Sanfilippo, J.E., Garczarek, L., Partensky, F., and Kehoe, D.M. (2019). Chromatic acclimation in cyanobacteria: a diverse and widespread process for optimizing photosynthesis. Annu. Rev. Microbiol. *73*, 407–433. https://doi.org/10.1146/annurev-micro-020518-115738.
42. Raszewski, G., and Renger, T. (2008). Light harvesting in photosystem II core complexes is limited by the transfer to the trap: can the core complex turn into a photoprotective mode? J. Am. Chem. Soc. *130*, 4431–4446. https://doi.org/10.1021/ja7099826.
43. Mohamed, A., Nagao, R., Noguchi, T., Fukumura, H., and Shibata, Y. (2016). Structure-based modeling of fluorescence kinetics of photosystem II: relation between its dimeric form and photoregulation. J. Phys. Chem. B *120*, 365–376. https://doi.org/10.1021/acs.jpcb.5b09103.
44. Chen, M., Donohoe, K., Crossett, B., Schliep, M., and Larkum, T. (2008). Molecular basis of antenna system adaptation in a chl *d*-containing organism. In Photosynthesis. Energy from the Sun, J.F. Allen, E. Gantt, J.H. Golbeck, and B. Osmond, eds. (Springer), pp. 243–246. https://doi.org/10.1007/978-1-4020-6709-9_54.
45. Oliver, T., Sánchez-Baracaldo, P., Larkum, A.W., Rutherford, A.W., and Cardona, T. (2021). Time-resolved comparative molecular evolution of oxygenic photosynthesis. Biochim. Biophys. Acta Bioenerg. *1862*, 148400. https://doi.org/10.1016/j.bbabio.2021.148400.
46. Chen, M., Bibby, T.S., Nield, J., Larkum, A.W.D., and Barber, J. (2005). Structure of a large photosystem II supercomplex from *Acaryochloris marina*. FEBS Lett. *579*, 1306–1310. https://doi.org/10.1016/j.febslet.2005.01.023.
47. Nagao, R., Ogawa, H., Tsuboshita, N., Kato, K., Toyofuku, R., Tomo, T., and Shen, J.-R. (2023). Isolation and characterization of trimeric and monomeric PSI cores from *Acaryochloris marina* MBIC11017. Photosynth. Res. *157*, 55–63. https://doi.org/10.1007/s11120-023-01025-x.
48. Hu, Q., Miyashita, H., Iwasaki, I., Kurano, N., Miyachi, S., Iwaki, M., and Itoh, S. (1998). A photosystem I reaction center driven by chlorophyll d in oxygenic photosynthesis. Proc. Natl. Acad. Sci. USA *95*, 13319–13323. https://doi.org/10.1073/pnas.95.22.13319.
49. Karapetyan, N.V., Bolychevtseva, Yu.V., Yurina, N.P., Terekhova, I.V., Shubin, V.V., and Brecht, M. (2014). Long-wavelength chlorophylls in photosystem I of cyanobacteria: origin, localization, and functions. Biochemistry (Mosc) *79*, 213–220. https://doi.org/10.1134/S0006297914030067.
50. Yang, D., Qing, Y., and Min, C. (2010). Incorporation of the chlorophyll d-binding light-harvesting protein from *Acaryochloris marina* and its localization within the photosynthetic apparatus of *Synechocystis* sp. PCC6803. Biochim. Biophys. Acta *1797*, 204–211. https://doi.org/10.1016/j.bbabio.2009.10.006.
51. Fossette, S., Abrahms, B., Hazen, E.L., Bograd, S.J., Zilliacus, K.M., Calambokidis, J., Burrows, J.A., Goldbogen, J.A., Harvey, J.T., Marinovic, B., et al. (2017). Resource partitioning facilitates coexistence in sympatric cetaceans in the California current. Ecol. Evol. *7*, 9085–9097. https://doi.org/10.1002/ece3.3409.
52. Golikov, A.V., Ceia, F.R., Sabirov, R.M., Batalin, G.A., Blicher, M.E., Gareev, B.I., Gudmundsson, G., Jørgensen, L.L., Mingazov, G.Z., Zakharov, D.V., et al. (2020). Diet and life history reduce interspecific and intraspecific competition among three sympatric Arctic cephalopods. Sci. Rep. *10*, 21506. https://doi.org/10.1038/s41598-020-78645-z.
53. Grant, P.R., and Grant, B.R. (2006). Evolution of character displacement in Darwin's finches. Science *313*, 224–226. https://doi.org/10.1126/science.1128374.
54. Nguyen, L.T., Schmidt, H.A., Von Haeseler, A., and Minh, B.Q. (2015). IQ-TREE: a fast and effective stochastic algorithm for estimating maximum-likelihood phylogenies. Mol. Biol. Evol. *32*, 268–274. https://doi.org/10.1093/molbev/msu300.
55. Darling, A.C.E., Mau, B., Blattner, F.R., and Perna, N.T. (2004). Mauve: multiple alignment of conserved genomic sequence with rearrangements. Genome Res. *14*, 1394–1403. https://doi.org/10.1101/gr.2289704.

56. Ishikawa, S.A., Zhukova, A., Iwasaki, W., and Gascuel, O. (2019). A fast likelihood method to reconstruct and visualize ancestral scenarios. Mol. Biol. Evol. *36*, 2069–2085. https://doi.org/10.1093/molbev/msz131.

57. Schliep, M., Crossett, B., Willows, R.D., and Chen, M. (2010). 18O labeling of chlorophyll d in *Acaryochloris marina* reveals that chlorophyll a and molecular oxygen are precursors. J. Biol. Chem. *285*, 28450–28456. https://doi.org/10.1074/jbc.M110.146753.

58. Li, Y., Scales, N., Blankenship, R.E., Willows, R.D., and Chen, M. (2012). Extinction coefficient for red-shifted chlorophylls: chlorophyll d and chlorophyll *f*. Biochim. Biophys. Acta *1817*, 1292–1298. https://doi.org/10.1016/j.bbabio.2012.02.026.

59. Felsenstein, J. (1981). Evolutionary trees from DNA sequences: a maximum likelihood approach. J. Mol. Evol. *17*, 368–376. https://doi.org/10.1007/BF01734359.

60. Hoang, D.T., Chernomor, O., von Haeseler, A., Minh, B.Q., and Vinh, L.S. (2018). UFBoot2: improving the ultrafast bootstrap approximation. Mol. Biol. Evol. *35*, 518–522. https://doi.org/10.1093/molbev/msx281.

61. Kalyaanamoorthy, S., Minh, B.Q., Wong, T.K.F., Von Haeseler, A., and Jermiin, L.S. (2017). ModelFinder: fast model selection for accurate phylogenetic estimates. Nat. Methods *14*, 587–589. https://doi.org/10.1038/nmeth.4285.

62. Gan, F., Zhang, S., Rockwell, N.C., Martin, S.S., Lagarias, J.C., and Bryant, D.A. (2014). Extensive remodeling of a cyanobacterial photosynthetic apparatus in far-red light. Science *345*, 1312–1317. https://doi.org/10.1126/science.1256963.

63. Graham, J.E., and Bryant, D.A. (2009). The biosynthetic pathway for Myxol-2′ Fucoside (Myxoxanthophyll) in the cyanobacterium *Synechococcus* sp. strain PCC 7002. J. Bacteriol. *191*, 3292–3300. https://doi.org/10.1128/JB.00050-09.

64. Eijckelhoff, C., and Dekker, J.P. (1997). A routine method to determine the chlorophyll a, pheophytin *a* and β-carotene contents of isolated photosystem II reaction center complexes. Photosynth. Res. *52*, 69–73. https://doi.org/10.1023/A:1005834006985.

Please cite this article in press as: Ulrich et al., Ecological diversification of a cyanobacterium through divergence of its novel chlorophyll *d*-based light-harvesting system, Current Biology (2024), https://doi.org/10.1016/j.cub.2024.05.022

STAR★METHODS

KEY RESOURCES TABLE

REAGENT or RESOURCE	SOURCE	IDENTIFIER
Bacterial and virus strains		
Acaryochloris marina MU03	Miller et al.[4]; NCBI	Accession: SAMN15662354
Acaryochloris marina WB4	Miller et al.[4]; NCBI	Accession: SAMN24371045
Acaryochloris marina GR1	Miller et al.[4]; NCBI	Accession: SAMN15662355
Acaryochloris marina MU08	Miller et al.[4]; NCBI	Accession: SAMN15662357
Acaryochloris marina MU09	Miller et al.[4]; NCBI	Accession: SAMN15662356
Acaryochloris marina MU05	Miller et al.[4]; NCBI	Accession: SAMN15662358
Acaryochloris marina CCMEE 5410	Miller et al.[4]; NCBI	Accession: GCA_000238775.2
Acaryochloris marina MU12	Miller et al.[4]; NCBI	Accession: SAMN15662360
Acaryochloris marina MU11	Miller et al.[4]; NCBI	Accession: SAMN15662359
Acaryochloris marina MU10	Miller et al.[4]; NCBI	Accession: SAMN15662361
Acaryochloris marina MU13	Miller et al.[4]; NCBI	Accession: SAMN15662362
Acaryochloris marina I2.1	Miller et al.[4]; NCBI	Accession: SAMN24371046
Acaryochloris marina MU07	Miller et al.[4]; NCBI	Accession: SAMN15662363
Acaryochloris marina MU06	Miller et al.[4]; NCBI	Accession: SAMN1566236
Acaryochloris marina MU04	Miller et al.[4]; NCBI	Accession: SAMN15662365
Acaryochloris marina NIES2412	Miller et al.[4]; NCBI	Accession: SAMN15662366
Acaryochloris marina Awaji	Miller et al.[4]; NCBI	Accession: SAMN15662367
Acaryochloris marina S1	Miller et al.[4]; NCBI	Accession: SAMN15662369
Acaryochloris marina S9	Miller et al.[4]; NCBI	Accession: SAMN15662370
Acaryochloris marina P4	Miller et al.[4]; NCBI	Accession: SAMN24371035
Acaryochloris marina P9	Miller et al.[4]; NCBI	Accession: SAMN24371036
Acaryochloris marina HP9	Miller et al.[4]; NCBI	Accession: SAMN15662371
Acaryochloris marina FH2	Miller et al.[4]; NCBI	Accession: SAMN24371038
Acaryochloris marina FH6	Miller et al.[4]; NCBI	Accession: SAMN24371039
Acaryochloris marina FH1	Miller et al.[4]; NCBI	Accession: SAMN24371037
Acaryochloris marina HP1	Miller et al.[4]; NCBI	Accession: SAMN15662372
Acaryochloris marina HP11	Miller et al.[4]; NCBI	Accession: SAMN24371044
Acaryochloris marina HP3	Miller et al.[4]; NCBI	Accession: SAMN24371041
Acaryochloris marina HP5	Miller et al.[4]; NCBI	Accession: SAMN24371042
Acaryochloris marina HP6	Miller et al.[4]; NCBI	Accession: SAMN24371043
Acaryochloris marina MSP2	Miller et al.[4]; NCBI	Accession: SAMN15662374
Acaryochloris marina HP10	Miller et al.[4]; NCBI	Accession: SAMN15662373
Acaryochloris marina S7	Miller et al.[4]; NCBI	Accession: SAMN15662377
Acaryochloris marina S15	Miller et al.[4]; NCBI	Accession: GCA_018336915.1
Acaryochloris marina HP8	Miller et al.[4]; NCBI	Accession: SAMN15662375
Acaryochloris marina FH11	Miller et al.[4]; NCBI	Accession: SAMN24371040
Acaryochloris marina MBIC11017	Swingley et al.[29]; NCBI	Accession: GCA_000018105.1
Acaryochloris thomasi RCC1774	Partensky et al.[32]; NCBI	Accession: NZ_PQWO00000000
Cyanothece sp. PCC7425	NCBI	Accession GCA_000022045.1
Prochlorococcus marinus str. AS9601	NCBI	Accession: PRJNA13548
Prochlorothrix hollandica PCC 9006	NCBI	Accession: PRJNA158811
Prochlorococcus marinus SS120	NCBI	Accession: PRJNA57995
Prochloron didemni	NCBI	Accession: PRJNA13452
Prochlorococcus marinus MED4	NCBI	Accession: PRJNA213

(*Continued on next page*)

Please cite this article in press as: Ulrich et al., Ecological diversification of a cyanobacterium through divergence of its novel chlorophyll *d*-based light-harvesting system, Current Biology (2024), https://doi.org/10.1016/j.cub.2024.05.022

Continued

REAGENT or RESOURCE	SOURCE	IDENTIFIER
Synechococcus sp. JA-3-3Ab	NCBI	Accession: PRJNA16251
Synechococcus sp. 65AY6Li	NCBI	Accession: PRJNA209725
Synechococcus sp. PCC 7335	NCBI	Accession: PRJNA19377
Fischerella sp. NIES-3754	NCBI	Accession: PRJDB4348
Synechococcus elongatus str PCC 7942	NCBI	Accession: PRJNA10645
Synechocystis sp. PCC 6803	NCBI	Accession: PRJNA715740
Synechococcus sp. PCC 7002	NCBI	Accession: PRJNA28247
Thermosynechococcus sp. NK55a	NCBI	Accession: PRJNA218025
Synechococcus sp. Nb3U1	NCBI	Accession: PRJNA795194
Miscellaneous Cyanobacterial Chlorophyll-binding proteins	NCBI	Accessions: PRJNA224116; PRJDB11069; PRJEB60184; PRJDB5665
Prochlorococcus Chlorophyll-binding proteins	NCBI	Accession: PRJNA246696
Biological samples		
Acaryochloris marina strains	University of Montana Culture Collection for Cyanobacteria	N/A
Deposited data		
Acaryochloris genome sequence data	Miller et al.[4]	NCBI BioProject: PRJNA649288
Software and algorithms		
IQ-TREE	Nguyen et al.[54]	V2.0
Mauve	Darling et al.[55]	V1
PastML	Ishikawa et al.[56]	V1.9.29.9
JMP	https://www.jmp.com/en_us/home.html	V17.2

RESOURCE AVAILABILITY

Lead contact

Further information and requests for resources and reagents should be directed to and will be fulfilled by the lead contact, Scott Miller (scott.miller@umontana.edu).

Materials availability

This study did not generate any new unique reagents.

Data and code availability

- This paper analyzes existing, publicly available data. These accession numbers for the datasets are listed in the key resources table.
- This paper does not report original code.
- Any additional information required to reanalyze the data reported in this paper is available from the lead contact upon request.

EXPERIMENTAL MODEL AND STUDY PARTICIPANT DETAILS

Acaryochloris culture maintenance

Acaryochloris strains were cultured in IO BG-11 or modified IO BG-11 media as in Ulrich et al.[5] Batch cultures containing 75 mL of media were maintained in 250 mL Erlenmeyer flasks at 20°C or 30°C under 12 h cycles of 20-25 μmol photons $m^{-2}s^{-1}$ cool white fluorescent light (350 – 800 nm). All strains are maintained in the University of Montana Culture Collection for Cyanobacteria and are available upon request.

METHOD DETAILS

Pigment extraction, room temperature spectroscopy, and tube assays

Absorbance scans were performed *in vivo* by first normalizing by optical density at 750 nm (OD_{750}) and measuring absorption from 300-800 nm with a Beckman Coulter DU 530 spectrophotometer (Indianapolis, IN). To calculate Chl *d* concentration, a methanol

assay was performed.[5,57] Briefly, 2 mL of culture were harvested and pelleted by centrifugation. The supernatant was discarded, and cell pellets were resuspended in 2 mL ice cold 100 % methanol. To extract pigments, samples were stored on ice in the dark for ~30 min, after which they were centrifuged to pellet cell debris. Chl *d* concentration (μg/ml) was determined by measuring the absorbance at 697 nm and then using the published extinction coefficient of Chl *d* in methanol (63.68 x 10^3 L $mol^{-1}cm^{-1}$; [58]). Aliquots of each culture were normalized by Chl *d* concentration before taking fluorescence emission spectra (450 nm excitation, 475-800 nm scan) with a Photon Technology International model QM-7/2005 spectrofluorometer (Ontario, Canada). Spectra were further normalized by peak wavelength.

Select *A. marina* strains were aliquoted into 15 mL of IOBG-11 media in culture tubes with a starting OD_{750} of 0.01. Tubes were propagated into different intensities of FR (0.94, 1.7, 3.5, and 10 μmol photons m^{-2} s^{-1}) and cool white light (15, 30, 46, 70, and 99 μmol photons m^{-2} s^{-1}) at 20°C. Metal screening was used to reduce light intensity. Pigments were extracted to normalize to Chl *d* concentration before fluorescence emission spectra were collected as above.

Phylogenetic analysis of A. marina LHC

The *Acaryochloris* spp. maximum likelihood phylogeny was used from Miller et al.,[4] with *Cyanothece* sp. PCC7425 (NCBI: GCA_000022045.1) as the outgroup. Ancestral state reconstruction was performed with PastML[56] using the marginal posterior probabilities approximation (MPPA) maximum likelihood model and F81 model for character evolution.[59] Amino acid sequences of *A. marina* Pcb obtained from annotated genome sequence assemblies in addition to other publicly available cyanobacterial Pcb, CP43, CP47, and IsiA protein sequences (NCBI: PRJNA224116, PRJNA13548, PRJNA158811, PRJNA57995, PRJNA13452, PRJNA213, PRJNA16251, PRJDB11069, PRJNA209725, PRJNA19377, PRJNA246696, PRJEB60184, PRJDB4348, PRJDB5665, PRJNA10645, PRJNA715740, PRJNA28247, PRJNA218025, PRJNA795194, PRJNA12997, PRJNA430151, and PRJNA649288) were used to create a concatenated alignment. The extrinsic loop between the 5th and 6th transmembrane helices was removed in PsbC (CP43) and CP47 sequences for better alignment to Pcb and IsiA proteins, which lack this large extrinsic loop.[45] We constructed a maximum likelihood tree with 1,000 ultrafast bootstrap replicates[60] using IQ-TREE version 2.0[54] according to the cpREV+F+I+G4 model of sequence evolution selected by the Akaike information criterion (AIC) in ModelFinder.[61] The Shimodaira-Hasegawa-like aLRT (SH-aLRT) was performed in parallel with bootstrap replicates to maximize load balance. To confirm presence/ absence of specific Pcb copies, we manually checked Pcb fragmented sequences for evidence of pseudogenization (premature stop codon) or artifacts from misalignment. The multiple genome alignment tool Mauve[55] was used to examine synteny of operons containing *pcb* copies. Gene trees of individual *pcb* copies were constructed from nucleotide alignments using the above method according to the TPM2u+F+G4, TIM2+F+G4, TIM2+F+G4 models of sequence evolution for *isiA*, *pcbA1* 1570 and *pcbA2* 1369 copies, respectively.

HPLC analysis

For HPLC analysis at The Pennsylvania State University, *A. marina* cells were harvested and washed once in 50 mM HEPES/NaOH buffer, pH 7.0 by gentle centrifugation, resuspension, and another centrifugation. Methods were followed as previously described.[62,63] Briefly, pigments were extracted from the cell pellet by sonication in acetone:methanol (7:2, v/v). Protein and other insoluble cell debris were removed by centrifugation, and pigment solutions were filtered through a 0.2-μm polytetrafluoroethylene membrane syringe filter. Next, pigments were analyzed by reversed-phase HPLC on a 25 cm • 4.6 mm analytical Discovery C18 column (Supelco, Bellefonte, PA, USA) using an Agilent Model 1100 HPLC system equipped with a model G1315B diode array detector. Chl ratios were estimated by calculating the area under each curve after normalizing to Pheophytin *a*. Pheophytin *a* is the primary electron acceptor of PSII and should not vary across strains.[64]

Membrane separation, fractionation, and spectroscopy

Cell pellets (5-8 g by dry weight) were stored in –80 °C and shipped to The Pennsylvania State University, University Park, for further processing. Pellets were resuspended in MES buffer containing 50mM MES (pH 6.5), 15 mM $CaCl_2$, and 10mM $MgCl_2$; 10 mL of buffer was used for each gram of cells. After homogenizing cells, a combination of approaches was used for cell lysis. Cells were passaged three times through a chilled French press (pressure ~ 138 MPa), sonicated, and passed through a microfluidizer (Microfluidics M-110EH-30 Microfluidizer Processor) at 30,000 psi. Further, a volume of 1 mL was mixed with an equal volume of 0.1-mm glass beads and cells were broken by eight rounds of 30 s of bead beating in a Mini-BeadBeater (BioSpec Products). Samples were centrifuged at 4000 rpm for 15 min in 10°C to remove cell debris. The supernatant was centrifuged at 40,000 rpm for 1 h in 4°C and pelleted membranes were resuspended in MES buffer. The Chl concentration was measured and adjusted to 0.4 mg Chl ml^{-1} by dilution with MES buffer. Membranes were then solubilized by addition of *n*-dodecyl-β-d-maltoside detergent (DM) to a final concentration of 1% (w/v) and incubated at 4°C for 1 h. Solubilized membranes were separated from insoluble debris by centrifugation at 8000 rpm for 15 min in 4°C. The solubilized membranes were loaded onto 5 to 20% (w/v) sucrose gradients containing 0.1% DM in MES buffer, and the gradients were centrifuged for about 18 hours at 108,000*g* in 4°C. Green-colored fractions were collected from sucrose gradients (see Figure 3A), dialyzed against MES buffer and concentrated using Millipore Centriprep 100K Centrifugal Filtration Devices (EMD Millipore, Darmstadt, Germany). For further purification, F2 and F3 fractions were loaded onto 5 to 20% (w/v) sucrose gradients containing 0.1% DM in MES buffer and subjected to a second ultracentrifugation for 18 hours at 108,000*g* in 4°C. Fractions were collected and dialyzed against MES buffer.

Please cite this article in press as: Ulrich et al., Ecological diversification of a cyanobacterium through divergence of its novel chlorophyll *d*-based light-harvesting system, Current Biology (2024), https://doi.org/10.1016/j.cub.2024.05.022

Absorption and low-temperature (77 K) fluorescence spectra were collected for membrane fractions after normalizing for Chl concentration. Absorption spectra (300-800 nm) were measured with Cary 14 spectrophotometer that was modified for solid-state operation by On-line Instrument Systems Inc. (Bogart, GA, USA). 77 K fluorescence emission spectra were measured using an SLM Model 8000C spectrofluorometer that has been modified for computerized solid-state operation by On-line Instrument Systems Inc., (Bogart, GA, USA). Membrane fractions were diluted in MES buffer to normalize Chl concentration and then glycerol was added to produce a final concentration of 60% (v/v). After loading into the measuring tube, samples were quickly frozen in liquid nitrogen. To measure the fluorescence emission from Chl-protein complexes, samples were excited at 450 nm and emission was measured over the range of 600-800 nm.

LC-MS Preparation

To precipitate the proteins from purified fractions, 12% PEG (w/v) was added to each tube, inverted to mix, and stored in 4°C overnight. The PEG/protein mixtures were centrifuged for 20 min at 30,000 rpm in 4°C. Supernatants were decanted, and pellets were briefly dried. The protein pellets were resuspended in resuspension buffer composed of 50 nM MES pH 6.5, 10 mM $MgCl_2$, 15 mM $CaCl_2$, 10 % glycerol, and 0.05% DM. Samples were stored in –80°C and prepared for LC-MS performed at the Penn State Proteomics and Mass Spectrometry Core Facility, University Park, PA.

FR growth and net oxygen production experiments

For each strain, triplicate independent cultures derived from the same inoculum were grown in 706 nm and 731 nm LED boxes in 25°C. The intensity of LED lights varied between 1.9-2.1 μmol photons $m^{-2}s^{-1}$. Growth was measured every 48 hours by taking OD_{750} readings of a 2 mL subsample, after which cultures were randomly moved to different positions within each respective light environment to mitigate any differences in light exposure. Growth rates (generations/day) were estimated from the exponential growth phase of each culture.

Aliquots of exponentially growing cells were gently homogenized and pelleted via low-grade centrifugation (5500*g* for 30 min) and resuspended in 2 mL IO BG-11 media to a normalized Chl *d* concentration. The sample was kept in the dark for at least 5 min prior to measuring net oxygen evolution with a Unisense OX-Eddy Clark-type oxygen sensor when the sample was exposed to 706 nm or 731 nm LED light for 30 sec. Each sample was measured twice and was dark acclimated as well as carefully homogenized with a sterile needle in between measurements. The oxygen sensor signal was recorded every second using the Unisense SensorSuite Logger software. Prior to experimental procedures, the oxygen sensor was calibrated following manufacturer's instructions for conversion from raw sensor signal (mV) to oxygen concentration (μmol O_2 L^{-1}). For each of the light treatments, the rate of oxygen evolution (μmol O_2 L^{-1} s^{-1}) was estimated by the initial slope of a stable increase of oxygen over 10-15 seconds.

QUANTIFICATION AND STATISTICAL ANALYSIS

Differences in growth rates and net rates of oxygen evolution of *A. marina* strains MU03, MU13, and HP10 in both light environments were assessed by linear models in JMP version 17.2 (SAS Institute Inc., Cary, NC). Details of other quantification analyses can be found in the results and discussion text.